

# Towards a Complete Multi-layered Framework for IEEE-802.11e Multi-hop Ad Hoc Networks\*

Rachid El-Azouzi<sup>1</sup>, Essaid Sabir<sup>1</sup>,  
Mohammed Raiss El Fenni<sup>1,2</sup>, and Sujit Kumar Samanta<sup>1</sup>

<sup>1</sup> LIA/CERI, University of Avignon, Agroparc BP 1228, Avignon, France

<sup>2</sup> LIMIARF, University of Mohammed V-Agdal, B.P. 1014 RP, Rabat, Morocco

{rachid.elazouzi,essaid.sabir}@univ-avignon.fr,

mohammed.raiss@etd.univ-avignon.fr,

sujitsamanta12@yahoo.com

**Abstract.** Performance of IEEE 802.11 in multi-hop wireless networks depends on the characteristics of the protocol itself, and on those of the other layers. We are interested in this paper in modeling the IEEE 802.11e Enhanced Distributed Coordination Function. This paper investigates the intricate interactions among PHY, MAC and Network layers. For instance, we jointly incorporate the carrier sense threshold, the transmit power, the contention window size, the retransmissions retry limit, the multi rates, the routing protocols and the network topology. Then, we build a general cross-layered framework to represent multi-hop ad hoc networks with asymmetric topology and asymmetric traffic. We develop an analytical model that predicts the throughput of each connection as well as the stability of forwarding queues at intermediate nodes. To the best of our knowledge, our work is the first to consider general topology and asymmetric parameters setup in PHY/MAC/Network layers. Performance of such a system is also evaluated via simulation. We show that the performance measures of MAC layer are affected by the traffic intensity of flows to be forwarded. More precisely, attempt rate and collision probability are dependent on the traffic flows, topology and routing.

**Keywords:** Ad hoc network, Performance Evaluation, Cross-layer architecture, Fixed point, Coupled systems.

## 1 Introduction

In next-generation wireless networks, it is likely that the IEEE 802.11 wireless LAN (WLAN) will play an important role and affect the style of people's daily life. People want voice, audio, and broadband video services through WLAN connections. Unlike traditional best effort data applications, multimedia applications require quality of service (QoS) support such as guaranteed bandwidth and bounded delay/jitter. There was a lot of interest in modeling the behavior

---

\* This work was partially sponsored by The Indo-French Center for the Promotion of Advanced Research under CEFIPRA Project #4000-IT-1.

of the IEEE 802.11 DCF (Distributed Coordination Function) and studying its performances in both the WLAN networks and the multi-hop context. Medium access control protocol has a large impact on the achievable network throughput and stability for wireless ad hoc networks. So far, the ad hoc mode of the IEEE 802.11 standard has been used as the MAC protocols for MANETs. This protocol is based on the CSMA/CA mechanism in DCF.

**Related Works and Their Drawbacks.** There have been a number of studies on the performance of IEEE 802.11 in ad hoc network. All these studies focus on MAC layer without taking into account the routing and the cooperation level of nodes in ad hoc networks, see e.g. [1, 2, 4, 8, 10–12]. A common point of those efforts was to extend Bianchi's model in saturated or unsaturated ad hoc network. Now, the problems of hidden terminals and the channel asymmetry become real issues. A non rare assumption is to consider implicitly symmetric traffic distribution or nodes randomly distributed on a plane following a Poisson point process. Hence, the collision probability and attempt rate are the same for all users. Yang et al. [12] propose an extension of Bianchi [3] model and characterize the channel activities from the perspective of an individual sender. They studied the impact of carrier sensing range and the transmit power on the sender throughput. The PHY/MAC impact was clearly considered. Basel et al. [1] were also interested in tuning the transmit power relatively to the carrier sense threshold. They provide a detailed comparison performance between the two-way and the four-way handshake. Medepalli et al. [8] propose an interesting framework model for analyzing throughput, delay and fairness characteristics of IEEE 802.11 DCF multi-hop networks. The applicability of the model in terms of network design is also presented.

**Aims of the Paper.** Our major aim is to build a complete framework to analyze multi-hop ad hoc networks under general and realistic considerations. We present a probabilistic but rigorous model incorporating jointly Network, MAC and PHY layers in a simple cross-layer architecture. This latter one has a potential synergy of information exchange among different layers, instead of the standard OSI non-communicating layers. Moreover, we consider the general case of topological asymmetric ad hoc networks in which the nodes have not the same channel perception and then the attempt rate may not always describe the real channel access. Moreover, this model is extended to the IEEE 802.11e which provides differentiated channel access to packets by allowing different rates and different back-off parameters. In order to handle QoS, several traffic classes are also supported. We also allow that each traffic may have different retry limits after which the packet is dropped. From analyzing the model, we find that the performance measures of MAC layer are affected by routing and the traffic intensity of flows to be forwarded. More precisely, the attempt rate and collision probability are now dependent on the traffic flows, topology and routing. Moreover, end-to-end throughput is independent of cooperation level when all forwarding queues are stable.

**Paper Organization.** We formulate the problem in Section 2. Then we derive the expression of end-to-end throughput and write a system that determines traffic intensities in the whole network in Section 3. We illustrate our results by some numerical examples in Section 4 and conclude the paper in Section 5. Due to the page limit, many details are omitted, we invite the reader to see our technical report [13].

## 2 Problem Formulation

### 2.1 Overview on IEEE 802.11 DCF/EDCF

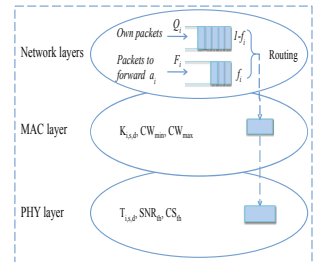
The distributed coordination function (DCF) of the IEEE 802.11 is based on the CSMA/CA protocol in which a node starts by sensing the channel before attempting any packet. Then, if the channel is idle it waits for an interval of time, called the Distributed Inter-Frame Space (DIFS), before transmitting. But, if the channel is sensed busy the node defers its transmission and waits for an idle channel. In addition, to reduce collisions of simultaneous transmissions, the IEEE 802.11 employs a slotted binary exponential back-off where each packet in a given node has to wait for a random number of time slots, called the back-off time, before attempting the channel. The back-off time is uniformly chosen from the interval  $[0, W - 1]$ , where  $W$  is the contention window that mainly depends on the number of experienced collisions. The contention window  $W$  is dynamic and given by  $W_i = 2^i W_0$ , where  $i$  represents the stage number (usually, it is considered as the current retransmission attempt number) of the packet, and  $W_0$  is the initial contention window. The back-off time is decremented by one slot each time when the channel is sensed idle, while it freezes if it is sensed busy. Finally, when the data is transmitted, the sender has to wait for an acknowledgement (ACK) that would arrive after an interval of time, called the Short Inter-Frame Space (SIFS). If the ACK is not received, the packet is considered lost and a retransmission has to be scheduled. When the number of retransmissions expires, the packet is definitively dropped. To consider multimedia applications, the IEEE 802.11e uses an enhanced mode of the DCF called the Enhanced DCF (EDCF) which provides differentiated channel access for different flow priorities. The main idea of EDCF is based on differentiating the back-off parameters of different flows. So, priorities can be distinguished due to different initial contention window, different back-off multiplier or different inter-frame space. An Arbitration IFS (AIFS) is used instead of DIFS. The AIFS can take at least a value of DIFS, then, a high priority flow needs to wait only for DIFS before transmitting to the channel. Whereas a low priority flow waits an AIFS greater than DIFS. In the next paragraph, we used a generalized model of the back-off mechanism.

### 2.2 Problem Modeling and Cross-Layer Architecture

The network layer of each node  $i$  handles two queues, see Figure 1. The forwarding queue  $F_i$  carries packets originated from some source nodes and destined to

some given destinations. The second one is  $Q_i$  which carries own packets of node  $i$  itself. We assume that the two queues have an infinite storage capacity. Packets are served with a first in first served fashion. When  $F_i$  is not empty, the node chooses to send a packet from  $F_i$  with a probability  $f_i$ , and it chooses to send from  $Q_i$  with probability  $1 - f_i$ . When one of these queues is empty we choose to send from the non empty queue with probability 1. When node  $i$  decides to transmit from the queue  $Q_i$ , it sends a packet destined to node  $d$ ,  $d \neq i$ , with probability  $p_{i,d}$ . This parameter characterizes somehow the QoS (Quality of Service) required by the initiated service from upper layers. We consider that each node has always packets to be sent from queue  $Q_i$ , whereas  $F_i$  maybe empty. Consequently, the network is considered saturated and mainly depends on the channel access mechanism. In ad hoc networks, each node behaves as a router. At each time, it has a packet to be sent to a given destination and starts by finding the next hop neighbor where to transmit the packet. Clearly, each node must carry routing information before sending the packet. Proactive routing protocols as the Optimized Link State Routing construct and maintain a routing table that carries routes to all nodes of the network. To do so, it has to send periodically some control packets. These kind of protocols correspond well with our model, especially since  $Q_i$  is non-empty. Here, nodes form a static network where routes between any source  $s$  and destination  $d$  are invariant. To consider routing in our model, we denote by  $R_{s,d}$  the set of nodes between a source  $s$  and destination  $d$  ( $s$  and  $d$  not included). Each node in our model can handle many connections on different paths. The traffic flow leaving a node  $i$  is determined by the channel allocation using IEEE 802.11 EDCF. However, differentiating the flow leaving  $F_i$  and the flow leaving  $Q_i$ , allows us to determine the load and the intensity of traffic crossing  $F_i$ . We denote here the probability that the forwarding queue  $F_i$  is non-empty by  $\pi_i$ . Similarly, we denote the probability that a packet of the path  $(s, d)$  is chosen in the beginning of a transmission cycle<sup>1</sup> by  $\pi_{i,s,d}$ . This quantity is exactly the fraction of traffic related to the path  $(s, d)$  crossing  $F_i$ , thus  $\pi_i = \sum_{s,d:i \neq s} \pi_{i,s,d}$ . We analyze in the following each layer separately and show how coupled they are and derive the metrics of interest.

**Fig. 1.** The interaction among Network, MAC and PHY layers is now clear. Attempting the channel begins by choosing the queue from which a packet must be selected. And then, this packet is moved from the corresponding queue at the network layer to the MAC layer where it will be transmitted according to the IEEE 802.11 DCF protocol. This manner, when a packet is in the MAC layer, it is attempted until it is removed from the node.



<sup>1</sup> A cycle is defined as the number of slots needed to transmit a single packet until its success or drop. It is formed by the four channel events seen by a sender. For instance : idle slots, busy slots, transmissions with collisions and/or a success.

**Accumulative Interference and Virtual Node:** During a communication between a sender node  $i$  and a receiver node  $j$  in a given path from  $s$  to  $d$  (where the source node of a connection is  $s$  and the destination node is  $d$ ), the node  $i$  transmits to  $j$  with a power  $T_{i,s,d}$ . The received power on  $j$  can be related to the transmitted one by the propagation relation  $T_{i,s,d} \cdot h_{i,j}$ , where  $h_{i,j}$  is the channel gain experienced by  $j$  on the link  $(i, j)$ . In order to decode the received signal correctly,  $T_{i,s,d} \cdot h_{i,j}$  should exceed the receiver sensitivity denoted by  $RX_{th}$ , i.e.,  $T_{i,s,d} \cdot h_{i,j} \geq RX_{th}$ . Under symmetry assumption and no accumulative effect of concurrent transmissions, the carrier sense range forms a perfect circle with radius  $r_1$ . Even when considering accumulative interference, the carrier sense can be reasonably approached by a circle with radius  $r_2 \geq r_1$ .

**Definition 1.** The group  $\mathcal{Z}$ , composed of nodes that cannot be heard individually by a sender  $i$  but their accumulative signal may jam the signal of interest, is called a **virtual node**. This way, the virtual node  $\mathcal{Z}$  is equivalent to a **fictional node** being in the carrier sense range of sender  $i$ .

We can then formulate the carrier sense set of a node  $i$  by the following expression

$$CS_i = \left\{ \mathcal{Z} : \forall s, d, k' \in \mathcal{Z}, \begin{array}{l} \sum_{k \in \mathcal{Z}} T_{k,s,d} \cdot h_{k,i} \geq CS_{th} \\ \sum_{k \in \mathcal{Z} \setminus k'} T_{k,s,d} \cdot h_{k,i} < CS_{th} \end{array} \right\}, \quad (1)$$

where  $CS_{th}$  is the carrier sense threshold. One can see  $CS_i$  as the set of virtual nodes that may be heard by sender  $i$  when it is sensing the channel in order to transmit on the path  $R_{s,d}$ . In other words,  $CS_i$  is the set of all real nodes (if they are neighbors of  $i$ ) and virtual nodes (due to accumulative interferences) that may interfere with node  $i$ . Now, we define  $H_{i,s,d}$  as the set of nodes that may sense the channel busy when node  $i$  is transmitting on the path  $(s, d)$ . Then

$$H_{i,s,d} = \{k : T_{i,s,d} \cdot h_{i,k} \geq CS_{th}, \forall s, d\}. \quad (2)$$

For sake of clarity, we are restricted in our formulation to the case of single transmission power. However, our model can be straightforwardly used for studying power control from nodes' individual points of view. An interesting feature is that when the transmission power level is the same for all nodes and accumulative interferences are neglected, we have  $CS_i = H_{i,s,d}$ . *Later result says that under considered assumptions, the set of nodes node  $i$  can hear is exactly the set of nodes that can hear node  $i$  when transmitting.* The receiver  $j_{i,s,d}$  can correctly decode the signal from sender node  $i$  if the Signal to Interference Ratio (SIR) exceeds a certain threshold  $SIR_{th}$ . Let the thermal noise variance, experienced on the path  $(s,d)$ , be denoted by  $N_{i,s,d}$ , then

$$SIR_{j_{i,s,d}} = \frac{T_{i,s,d} \cdot h_{i,j}}{\sum_{k \neq i} T_{k,s',d'} \cdot h_{k,j} + N_{i,s,d}} \geq SIR_{th}, \quad \forall s, d, s', d'. \quad (3)$$

We define now the interference set of a receiver  $j_{i,s,d}$  in a path  $(s,d)$ , denoted by  $\mathcal{T}_{j_{i,s,d}}$ , as the collection of its virtual nodes, i.e., all combination of nodes whose the accumulative signal may cause collisions at  $j_{i,s,d}$ . For instance, the virtual node  $\mathcal{Z}$  is in the interference set of node  $j_{i,s,d}$  iff the received signal from node  $i$  is completely jammed when nodes in  $\mathcal{Z}$  are transmitting all together. The interference set of node  $j$  is then written as

$$\mathcal{T}_{j_{i,s,d}} = \left\{ \mathcal{Z} : \begin{array}{l} \frac{T_{i,s,d} \cdot h_{i,j}}{\sum_{z \in \mathcal{Z}} T_{z,s',d'} \cdot h_{z,j} + N_{i,s,d}} < SIR_{th}, \\ \frac{T_{i,s,d} \cdot h_{i,j}}{\sum_{z \in \mathcal{Z} \setminus z'} T_{z,s',d'} \cdot h_{z,j} + N_{i,s,d}} \geq SIR_{th}, \\ \forall z', s', d', z' \neq i, s' \neq s, d' \neq d. \end{array} \right\} \quad (4)$$

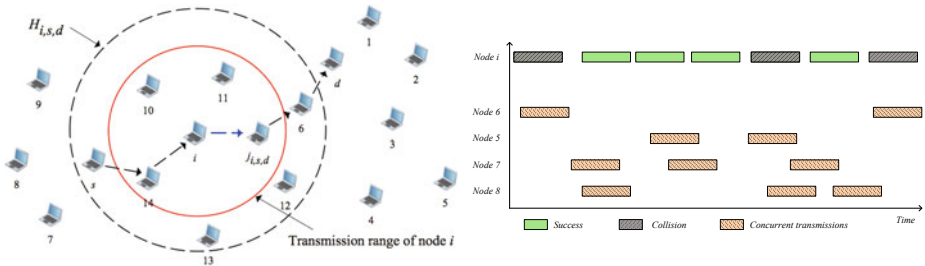


**Fig. 2.** Those plots show the transmission range of node  $i$  and the set of real nodes  $H_{i,s,d}$  that can hear  $i$  when transmitting to node  $j_{i,s,d}$ . The carrier sense  $CS_i$  of node  $i$  and the interference set  $\mathcal{T}_{j_{i,s,d}}$  are not plotted because they depend on transmit powers of all nodes in the network as well as the topology and scale of the network. For instance  $H_{i,s,d} = \{\{s\}, \{j_{i,s,d}\}, \{6\}, \{10\}, \{11\}, \{12\}, \{13\}, \{14\}, \{7, 8, 9\}, \{d, 4\}, \{1, 5, 7, 8\}, \dots\}$

Figure 2 shows explicitly two different areas that need to be considered when a couple of nodes are communicating. Here, we distinguish (i) the transmission area where two nodes can send and receive packets mutually, (ii) the set of nodes that may hear ongoing transmissions of node  $i$ , and (iii) implicitly the carrier sense area where two nodes may hear each other but cannot decode the transmitted data. In Figure 2, we have situated the communication of  $i$  and  $j$  on the path  $(s,d)$ , so we can integrate the impact of the routing in the model. Figure 2 illustrates the effect of accumulative interference on transmission cycles of node  $i$ . For illustrative purpose, we consider the following virtual nodes :  $\{6\}$  and  $\{5, 7, 8\}$ . Node 6 is a neighbor of receiver  $j$  which causes collision whenever they both, i.e., nodes  $i$  and 6, are transmitting simultaneously. Whereas a failure may only occur when nodes of virtual node  $\{5, 7, 8\}$  are all transmitting altogether with sender  $i$ .

Each node uses the IEEE 802.11 DCF to access the channel and each one can use different back-off parameters. Let  $K_{i,s,d}$  be the maximum number of

transmissions allowed by a node  $i$  per packet on the path  $(s, d)$ . Then after  $K_{i,s,d}$  number of transmissions the packet is dropped. Also let  $p_i$  be the back-off multiplier of a given node  $i$ . The maximum stage number of node  $i$  is obtained from  $W_{m,i} = p_i^{m_i} W_{0,i}$ , where  $W_{m,i}$  and  $W_{0,i}$  are, respectively, the maximum and initial contention window for node  $i$ . If  $K_{i,s,d} < m_i$  then  $m_i$  takes the value of  $K_{i,s,d}$ , otherwise  $m_i = \log_{p_i} \left( \frac{W_{m,i}}{W_{0,i}} \right)$ . Using a contention window  $W_{k,i}$  for stage  $k$  of node  $i$ , the average back-off time for this stage is  $b_{k,i}$ . Remark that back-off parameters of different nodes may be different. Then, the system of nodes are nonhomogeneous as defined by [9].

We consider the modeling problem of the IEEE 802.11 using the perspective of a sender which consists on the channel activity sensed by a sender, or on the state (success or collision) of its transmitted packet. This will facilitate the problem in the ad hoc environment where nodes have an asymmetric vision of the channel. We start by defining the notion of virtual time slot and channel activity, then we write the expression of the attempt probability for the asymmetric topology. Consider that time is slotted with a physical slot duration  $\tau$ . Nodes transmit in the beginning of each slot and the transmission duration depends on the kind of the transmitted packet. A data packet has a fixed length and takes *Payload* (integer) slots to be transmitted (it includes the header transmission time). While an acknowledgment packet spends *ACK* slots. In our model we consider the two-way handshaking scheme, but it is easily extended to the four-way handshaking scheme. On one hand, a sender node before transmitting would see the channel either **busy** or **idle**. On the other hand, its transmitted packet may encounter a **success** or a **collision**. These four states define all the possibilities that a sender may observe. Therefore, the average time spent in a given state (seen by this sender) will be referred as the **virtual slot** of this sender. A remarkable feature here is that this virtual time would depend on the receiver, i.e., on the path where the packet is transmitted. In fact, the success or the collision of the transmitted packet is itself function of the actual receiver interferences state. For that, we denote by  $\Delta_{i,s,d}$  the virtual slot seen by node  $i$  on the path  $(s, d)$  that we will derive later on. Considering any asymmetric topology, we will always note the metrics functions of the path chosen for transmission. We recall that when we mention the node  $j_{i,s,d}$ , it will be clear that this is the receiver of node  $i$  on the path  $(s, d)$ .

At steady state and such as [3], we use the key assumption which states that at each transmission attempts, and regardless of the number of retransmissions suffered, each packet collides with constant and independent probability. However, collisions may depend only on the receiver channel state. For that we denote by  $\gamma_{i,s,d}$  the probability that a transmission of a packet of relay  $i$  on the path  $(s, d)$  fails due to either a corruption of the data or of its acknowledgment. Thus,  $(1 - \gamma_{i,s,d})$  is the probability of success in the path  $(s, d)$ . Henceforth, the attempt probability seen by a sender also depends on the receiver, and the well known formula of [3] can be used in the ad hoc network as confirmed in [12]. However, in the asymmetric network the attempt probability ( $P_{i,s,d}$ ) (in a virtual slot) for a node  $i$  will be different for each path  $(s, d)$  and can be written as in [6]:

$$P_{i,s,d} = \frac{1 + \gamma_{i,s,d} + \gamma_{i,s,d}^2 + \cdots + \gamma_{i,s,d}^{K_{i,s,d}-1}}{b_{0,i} + \gamma_{i,s,d} b_{1,i} + \gamma_{i,s,d}^2 b_{2,i} + \cdots + \gamma_{i,s,d}^{K_{i,s,d}-1} b_{K_{i,s,d}-1,i}} \quad (5)$$

where  $b_{k,i} = (p_s^k W_{0,i} - 1)/2$ . In the average, a node  $i$  will attempt the channel (for any path  $(s, d)$ ) with a probability  $P_i$  which mainly depends on the traffic and the routing table (here, it is maintained by OLSR protocol). Then

$$P_i = \sum_{s,d:i \in R_{s,d}} \pi_{i,s,d} f_i P_{i,s,d} + \sum_d (1 - \pi_i f_i) p_{i,d} P_{i,i,d}. \quad (6)$$

Similarly, the average virtual slot seen by node  $i$  is written

$$\Delta_i = \sum_{s,d:i \in R_{s,d}} \pi_{i,s,d} f_i \Delta_{i,s,d} + \sum_d (1 - \pi_i f_i) p_{i,d} \Delta_{i,i,d}. \quad (7)$$

*Remark 1.* The attempt probability (or attempt rate) must be differentiated from the transmission probability. This refers to the probability that a node transmits at any slot. Therefore, the transmission probability, if found, can characterize the channel allocation per node. In WLAN, it is sufficient to analyze the back-off rate to determine the channel allocation rate.

Note that  $1 - \pi_i f_i$  is the probability to find a packet from  $Q_i$  in the MAC layer. It seems important to note that the attempt probability represents the back-off expiration rate. It is the transmission probability in an idle slot (only when the channel is sensed idle). For that, it is convenient to work with MAC protocols that are defined by only an attempt probability, this kind of definition may englobe both slotted Aloha and CSMA type protocols including IEEE 802.11. The problem in ad hoc is that nodes have not the same channel vision (or different back-off parameters) and then the attempt probability may not always describe the real channel access. In [9], the problem of short term unfairness was studied in the context of a WLAN.

**Collision Probability and Virtual Slot Expressions.** The collision probability of a packet occurs when either the data or the acknowledgment experiences a collision. If we note by  $\gamma_{i,s,d}^D$  and  $\gamma_{j_i,s,d,s,d}^A$ , respectively, the collision probability of a data packet and its acknowledgement, then we have

$$\gamma_{i,s,d} = 1 - (1 - \gamma_{i,s,d}^D) (1 - \gamma_{j_i,s,d,s,d}^A), \quad (8)$$

The attempt probability of a virtual node  $\mathcal{Z}$  is defined by  $P_{\mathcal{Z}} = \prod_{z \in \mathcal{Z}} P_z$ . Therefore, the virtual slot of a virtual node  $\Delta_{\mathcal{Z}}$  can be reasonably estimated using the minimum virtual slot among all nodes in  $\mathcal{Z}$ , i.e.,  $\Delta_{\mathcal{Z}} = \min_{j \in \mathcal{Z}} \Delta_j$ . Thus the probability that transmitted data collides with other concurrent transmissions can be written as

$$\gamma_{i,s,d}^D = 1 - \prod_{k \in H_{i,s,d} \cap \mathcal{T}_{j_i,s,d}} (1 - P_k) \left( 1 - \sum_{\mathcal{Z} \in \mathcal{T}_{j_i,s,d} \setminus H_{i,s,d}} P_{\mathcal{Z}} \frac{\text{Payload}}{\Delta_{\mathcal{Z}}} \right). \quad (9)$$



Indeed, nodes in area  $H_{i,s,d} \cap \mathcal{T}_{j,i,s,d}$  must be silent at the beginning of node  $i$  transmission. While nodes in  $\mathcal{T}_{j,i,s,d} \setminus H_{i,s,d}$  are hidden to  $i$  (they constitute the virtual nodes of  $i$ ) and needs to be silent during all the data transmission time which is a vulnerable time. The  $\frac{Payload}{\Delta_j}$  is the normalized vulnerable time. After the beginning of data transmission, nodes in  $H_{i,s,d}$  will defer their transmission to *EIFS* (Extended Inter-Frame Space) duration, which would insure the good reception of the acknowledgement. In practice, acknowledgement are small packets and less vulnerable to collision, for that it is plausible to consider  $\gamma_{j,i,s,d,s,d}^A \simeq 0$ . Then, we can write  $\gamma_{i,s,d} = \gamma_{i,s,d}^D$ .

Considering the previously defined four states and from node  $i$  view, the network stays in a single state a duration equal to  $\Delta_{i,s,d}$ . It's given by

$$\Delta_{i,s,d} = P_{i,s,d}^{succ}.T_{succ} + P_{i,s,d}^{col}.T_{col} + P_i^{idle}.T_{idle} + P_i^{busy}.T_{busy}, \quad (10)$$

where  $T_{succ} = Payload + ACK + SIFS + DIFS$ ,  $T_{col} = Payload + ACK + DIFS$ ,  $T_{idle} = \tau$ ,  $T_{busy} = Payload + DIFS$ ,  $P_{i,s,d}^{succ} = P_{i,s,d}(1 - \gamma_{i,s,d})$ ,  $P_{i,s,d}^{col} = P_{i,s,d}\gamma_{i,s,d}$ ,  $P_i^{idle} = \prod_{\mathcal{Z} \in CS_i \cup \{i\}} (1 - P_{\mathcal{Z}})$ , and  $P_i^{busy} = (1 - P_i) \sum_{\mathcal{Z} \in CS_i} P_{\mathcal{Z}}$ .

Finally, let us denote the equations (5), (6), (8) and (10) by *system I*. Normally, it is sufficient to solve the *system I* to derive the fixed points of each node. However, by introducing the traffic metric in equations (6) and (7), these equations cannot be solved without knowing the  $\pi_{i,s,d}$  which is defined as the traffic intensity for each path  $(s, d)$  crossing node  $i$ . Therefore, in Section 3, we proceed in writing the rate balance equations at each node, from which  $\pi_{i,s,d}$  can be derived function of  $P_j$  and  $\gamma_{j,s,d}$ , for all  $j$ . These rate balance equations that give the traffic intensities. The problem resides in the complexity of the systems and in the computational issue.

### 3 End-to-End Throughput and Traffic Intensity System

We are interested in this section to derive the end-to-end throughput per connection, function of different layer parameters, including the IEEE 802.11 parameters. It is clear that the average performance of the system is hardly related to the interaction PHY/MAC/NETWORK. We focus now on the traffic crossing the forwarding queues, which may be an issue on the buffers stability. We say that a queue  $F_i$  is stable if the departure rate of packets from  $F_i$  is equal to the arrival rate into it. This is a simple definition of stability that can be written with a *rate balance equation*. We are going to derive this equation for each node  $i$  and each connection  $(s, d)$ . The system of these equations, for all  $i$  and  $(s, d)$ , will form the traffic intensities system, it will be referred as *system II*. In sum, we are writing a system that determines  $\pi_{i,s,d}$  for all  $i$  and  $(s, d)$ . For that, we first derive the average length of a transmission cycle per packet  $C_i$  at node  $i$ , see [13] for detailed computation. Then we write the departure rate from  $F_i$  as well as the arrival rate into it.

**Departure Rate:** The departure rate from  $F_i$  is the probability that a packet is removed from node  $i$  (forwarding queue) by either a successful transmission or a drop after successive  $K_{i,s,d}$  failures. The departure rate concerning only the packets sent on the path  $R_{s,d}$  is denoted by  $d_{i,s,d}$ . Formally, for any node  $i$ ,  $s$  and  $d$  such that  $p_{s,d} > 0$  and  $i \in R_{s,d}$ , the long term departure rate of packets from node  $i$  on the route from  $s$  to  $d$  is given by the following theorem:

**Theorem 1.** The long term departure rate from node  $i$  related to path  $R_{s,d}$  is given by

$$d_{i,s,d} = \frac{f_i \pi_{i,s,d}}{C_i}. \quad (11)$$

*Proof.* The reader is referred to [13] for a detailed proof.

Hence, it is easy to derive the total departure rate  $d_i$  on all paths:

$$d_i = \sum_{s', d': i \in R_{s', d'}} d_{i, s', d'} = \frac{\pi_i f_i}{C_i}.$$

**Arrival Rate and End-to-End Throughput:** The probability that a packet arrives to the queue  $F_i$  of the node  $i$  is also called the arrival rate, we denote it by  $a_i$ . When this rate concerns only packets sent on the path  $R_{s,d}$ , we denote it by  $a_{i,s,d}$ . Formally, for any nodes  $i$ ,  $s$  and  $d$  such that  $p_{s,d} > 0$  and  $i \in R_{s,d}$ , the long term arrival rate of packets into  $F_i$  for  $R_{s,d}$  is provided by the following

**Theorem 2.** The long term arrival rate into node  $i$  forwarding queue, related to path  $R_{s,d}$ , is given by

$$a_{i,s,d} = (1 - \pi_s f_s) \cdot \frac{p_{s,d}}{C_s} \cdot \prod_{k \in R_{s,i} \cup s} \left(1 - \gamma_{k,s,d}^{K_{k,s,d}}\right). \quad (12)$$

*Proof.* The reader is referred to [13] for a detailed proof.

**End-to-End Throughput:** The global arrival rate at  $F_i$  is  $a_i = \sum_{s,d: i \in R_{s,d}} a_{i,s,d}$ . Remark that when the node  $i$  is the final destination of a path  $R_{s,d}$ , then  $a_{d,s,d}$  represents the end-to-end average throughput of a connection from  $s$  to  $d$ . Practically,  $a_{d,s,d}$  is the number of delivered (to destination) packet per slot. Let  $\rho$  be the bit rate in bits/s of the wireless network. Therefore, the throughput in bits/s can be written as follows:

$$thp_{s,d} = a_{d,s,d} \cdot \text{Payload} \cdot \rho. \quad (13)$$

**Rate Balance Equations/Traffic Intensity System:** Finally, in the steady state if all the queues in the network are stable, then for each  $i$ ,  $s$  and  $d$  such that  $i \in R_{s,d}$  we get  $d_{i,s,d} = a_{i,s,d}$ , which is the rate balance equation on the path  $R_{s,d}$ . For all  $i$ ,  $s$  and  $d$  we get the traffic intensity system: *system II*. And when we sum the both sides of this last system, we get the global rate balance equation:  $d_i = a_i$ .

Let  $y_i = 1 - \pi_i f_i$  and  $z_{i,s,d} = \pi_{i,s,d} f_i$ . Thus  $y_i = 1 - \sum_{s,d:i \in R_{s,d}} z_{i,s,d}$ . Then, the rate balance equation can be written in the following form:

$$\sum_{d:i \in R_{s,d}} z_{i,s,d} = \frac{y_s (\sum_{s',d'} z_{i,s',d'} \hat{C}_{i,s',d'} + \sum_{d''} y_i p_{i,d''} \hat{C}_{i,i,d''}) w_{s,i}}{(\sum_{s',d'} z_{s,s',d'} \hat{C}_{s,s',d'} + \sum_{d''} y_s p_{s,d''} \hat{C}_{s,s,d''})}, \quad (14)$$

where  $w_{s,i} = \sum_{d:i \in R_{s,d}} p_{s,d} \prod_{k \in R_{s,i} \cup s} (1 - \gamma_{k,s,d}^{K_{k,s,d}})$ .

An interesting interpretation and application of equation (14) are the following: (i)  $z_{i,s,d}$  and  $y_i$  (can be considered as the stability region of node  $i$ ) are independent of the choice of  $f_i$ . (ii) For some values of  $f_i$  the forwarding queue of node  $i$  will be stable. Concerning  $P_i$ , we notice that it can be written as  $P_i = \sum_{s,d:i \in R_{s,d}} z_{i,s,d} P_{i,s,d} + \sum_d y_i p_{i,d} P_{i,i,d}$ . Then it depends on  $z_{i,s,d}$  and  $y_i$ , but it is not affected by  $f_i$ . A similar deduction is also observed for the energy consumed when sensing the channel or transmitting data. It turns out to be independent of the choice of cooperation level  $f_i$ . Hence, the node can fine-tunes  $f_i$  to improve the expected delay without affecting the throughput or the energy consumption. The reader is referred to our technical report [13] for detailed comments and derivation of the average energy. We have also developed an algorithm to jointly solve *System I* and *System II*, see algorithm 1 in our detailed technical report [13].

## 4 Simulation and Numerical Investigations

We turn in this section to study a typical example of multi-hop ad hoc networks. We consider a simple network formed by 9 nodes, identified using an integer from 1 to 9 as shown in Fig. 3. We establish 9 flows (or connections) labeled by a letter from  $a$  to  $i$ . Each node is located by its plane Cartesian coordinates expressed in meters. Except contraindication, the main parameters are fixed as follows:  $CW_{min} = 32$ ,  $CW_{max} = 1024$ ,  $K_{i,s,d} \equiv K = 5$ ,  $f_i \equiv f = 0.9$  (to insure operating in the stability region of all forwarding queues),  $T_{i,s,d} \equiv T = 0.1W$  ( $\forall i, s, d$ ),  $CS_{th} = 0$  dBm,  $RX_{th} = 0$  dBm,  $SIR_{th} = 10$  dB (target SIR),  $\rho = 2$  Mbps (bit rate),  $\tau = 20\mu s$  (physical slot duration),  $DISF = 3\tau$  and  $SIFS = \tau$ . For sake of illustration, we assume that the signal attenuation is only due to the path-loss phenomenon, i.e., a receiver  $j$  experiences a signal power of  $c \cdot T_{i,s,d} \cdot d_{i,j}^{-\alpha}$ , where  $\alpha = 2$  (path-loss exponent) and  $c = 6$  dBi (antenna gain).

**Model Validation:** We first perform extensive numerical and simulation examples to show the accuracy of our model and then study the impact of joint PHY/MAC/NETWORK parameters. For that aim, a discrete time simulator that implements the IEEE 802.11 DCF, integrating the weighted fair queueing over the two buffers previously discussed, is used to simulate the former network. Each simulation is run out during  $10^6$  physical slots, repeated at least 20 times and then averaged to smooth out the fluctuations caused by random numbers generator of the simulator (back-off counters). We checked the validity of the model by extensively considering different network scenarios (different flows and nodes parameters), several topologies (linear, circular and arbitrary topologies)

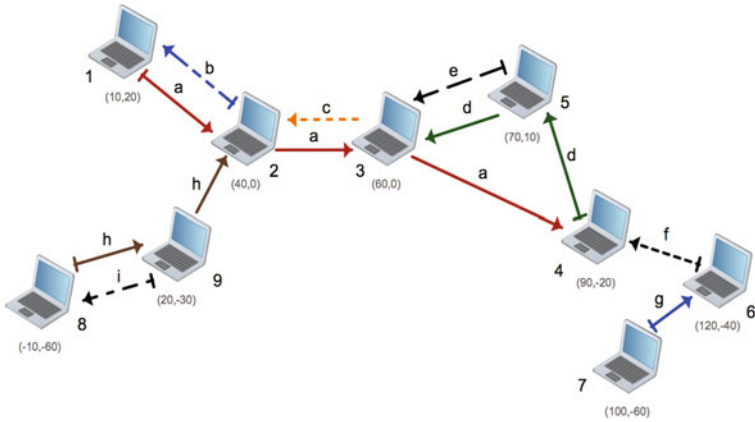


Fig. 3. The multi-hop ad hoc network used for simulations

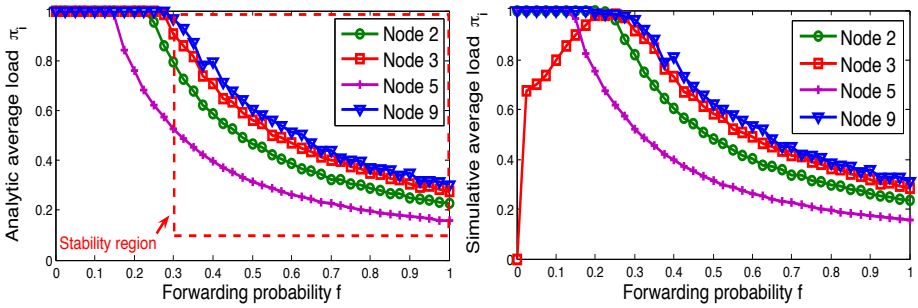


Fig. 4. Average forwarding queues load versus forwarding probability

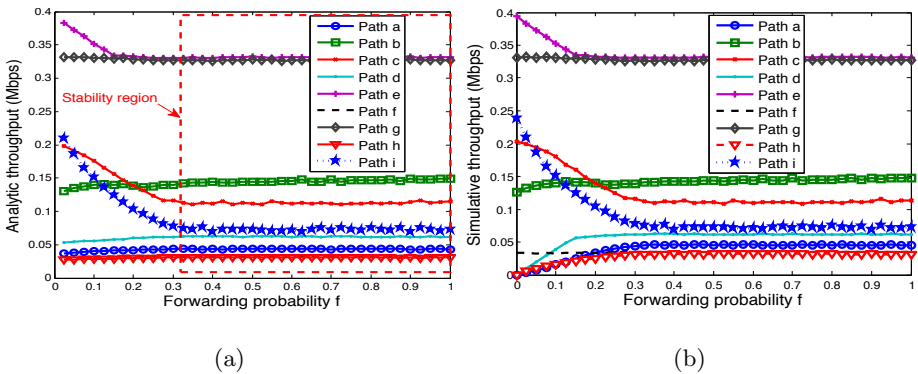
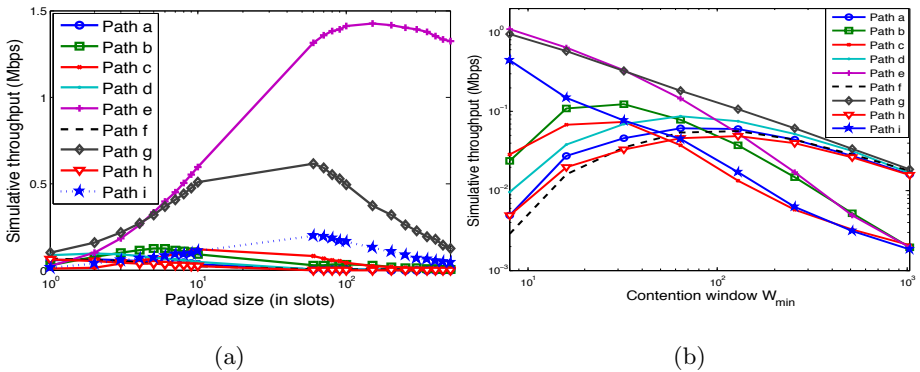


Fig. 5. Average e2e throughput versus the forwarding probability

and different network population size. We depict in Fig. 4(a) and Fig. 4(b) the analytic and the simulated average load  $\pi_i$  of forwarding queues respectively. Numerical plots show that analytic model match well with simulated results. Accuracy is particularly high under the stability region which is the main applicability region of our model. We refer to the interval of forwarding probability that insures a load strictly less than 1 for all queues, as the stability region of the system. The main difference seen between individual loads is mainly due to the topology asymmetry. Based on Fig. 5 (a) and (b), we note that our analytic finding, saying that *under the stability condition, the end-to-end throughput does not depend on the choice of the WFQ weight* (i.e., the cooperation level or also the forwarding probability  $f$ ), is confirmed. Therefore, one can *judiciously fine-tune the cooperation level value to decrease the delay while the average throughput remains almost constant*. This mechanism may play a crucial role in delay sensitive traffic support over multi-hop networks. One can note that the system stability region is strongly impacted by the nodes density. Indeed, in regions with relatively high or high nodes density, it is crucial that relay nodes should become more cooperative to insure their stability. Otherwise, the waiting of packet in forwarding queues may grow drastically and the network reliability becomes a hard issue.



**Fig. 6.** Average e2e throughput versus payload and contention window

Interested reader is referred to [13] for more details, extensive simulations and complete performance evaluation in terms of the considered cross-layer architecture. For instance many results on how to set values of  $CW_{min}$ , Payload size and other nodes intrinsic parameters were discussed. We first stipulate that an optimal payload size may not exist, see Fig. 6(a). Indeed, we note that some specific payload size is providing good performances in term of average throughput over some paths, but may hurt drastically the throughput on other links and then the reachability becomes a real issue. *Setting the payload size to a fixed value over the whole network is, in general, unfair and is not suitable for multi-hop networks*. However fortunately, locally optimal payload size may exist. This way, it depends strongly on the topology and the local node densities, i.e., the number

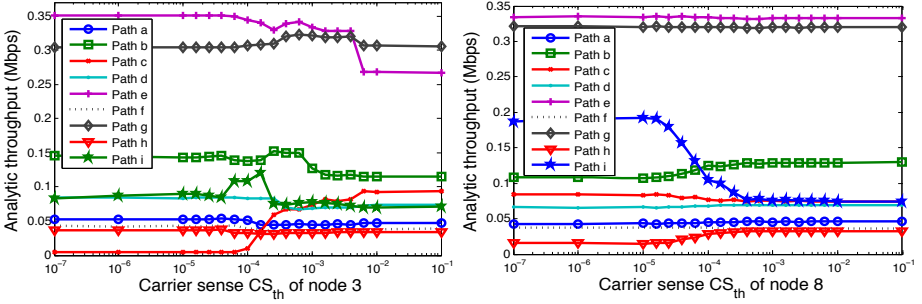


Fig. 7. End-to-end throughput versus carrier sense threshold (in Watt)

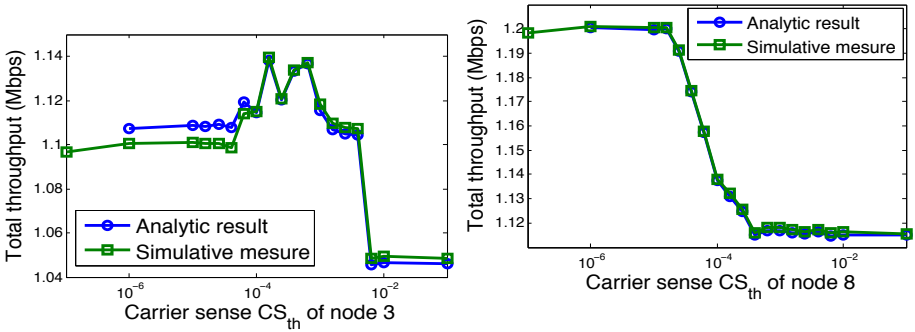
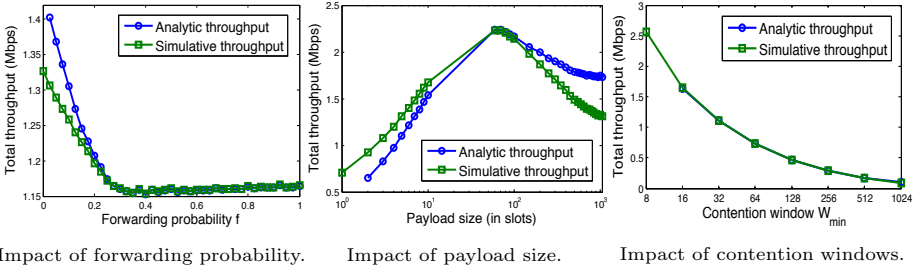


Fig. 8. Total throughput versus carrier sense threshold (in Watt)

of neighbors per  $m^2$ , their respective distances with respect to a node and how they are distributed in the network. In terms of the minimum contention window  $CW_{min}$ , see Fig. 6(b), the throughput has two different behaviors. Indeed, when the nodes density is low, the throughput is maximized for short backlog duration. Here, nodes tend to transmit more *aggressively*, having a relatively low collision probability due to low number of competitors. We also note that contention windows tends to increase as the nodes density becomes high. This statement is quite intuitive and due to the competitions that becomes colossal. In terms of queues load (equivalently delay), it is clear that when the contention windows increases it implies the increase of queues load, thus node may suffer from huge delay.

**Per Path Power and Carrier Sense Control:** We can reconsider here the Spanning tree-based algorithm proposed in [7] to compute the optimal transmit power for each path. *Each node sets its transmit power to a level that allows reaching the farthest neighbor*, i.e., the received power is at least equal to the receiver sensitivity. Consequently, this per path power control may improve the spatial reuse. In order to analyze the impact of carrier sense threshold on network performances, we vary  $CS_{th}$  for some node and fix it to the default value



**Fig. 9.** The system total throughput under different parameters variation

for remaining nodes, i.e.,  $CS_{th} = 0$  dBm. We plot in Fig. 7 the average throughput on all paths when tuning the carrier sense threshold of node 3 which is located in a relatively dense zone. The throughput of all connections continues to decrease (in particular connections crossing node 3 or its immediate neighbors) with  $CS_{th}$  except connections originated from node 3. Now we analyze the interplay of node 8 (in a low dense zone) carrier sense on network throughput. We note that the only negatively impacted connection is the connection  $i$  originated from node 9 (immediate neighbor of node 8). When carrier sense of node 8 is increasing, it becomes more nose-tolerant which implies high transmission aggressiveness. Which explains the throughput decrease of connection  $i$ . Thus connections crossing neighbors of node 9 take benefit from the low attempt rate of node 9 to improve their throughput, for instance connections  $a$ ,  $b$  and  $h$ .

**Aggregate Throughput:** In terms of total capacity, see Fig. 8, and depending on the local nodes density, the carrier sense control may increase the network capacity. Indeed, when a node in a dense zone fine-tunes its carrier sense threshold, we note existence of a region where the total capacity is maximized. This region correspond to a  $CS_{th}$  interval where node benefits from relatively high throughput and other nodes don't suffer much. Whereas, it seems that tuning carrier sense by nodes in low dense parts of the network may cause a throughput decrease. To sum up, we can say that on one hand, a higher carrier sense threshold encourages more concurrent transmissions but at the cost of more collisions. On the other hand, a lower carrier sense threshold reduces the collision probability but it requires a larger spatial footprint and prevents simultaneous transmissions from occurring, which may result in limiting the system capacity. Analyzing Fig. 9 where the behavior of the total capacity is depicted as a function of nodes intrinsic parameters ( $f_i$ ,  $Payload_i$  and  $CW_{min}$ ) we note the following : As expected from equation (14), the total capacity is insensitive for all cooperation level in the stability region. However, the cooperation is crucial to maintain the network connectivity. In terms of minimum contention window it seems that a as the  $CW_{min}$  increases as the total capacity decreases, and an optimal payload length that maximizes the total capacity may exist. More discussions are available in the full version [13].

## 5 Conclusion

In multi-hop ad hoc networking, a stack of protocols would interact with each other to accomplish a successful packet transfer. In this context, we have developed a cross-layered model built on the IEEE 802.11e EDCF standard. We studied the effect of forwarding on end-to-end performances. We have discovered that the modeling of the IEEE 802.11 in this context is not yet mature in the literature and to the best of our knowledge, there is no study done that considers jointly the PHY/MAC/NETWORK interaction in a non-uniform traffic and a general network topology. This has led us to build a general framework using the perspective of individual senders. The attempt and collision probabilities are now functions of the traffic intensity, on topology and on routing decision. The fixed point *system I* is indeed related to the traffic intensity *system II*. This paper opens many interesting directions to study in future such as power control and delay-based admission control with guaranteed throughput. Moreover, we will deal with the issue of cooperation between node in a game theoretical perspective.

## References

1. Alawieh, B., Assi, C., Mouftah, H.T.: Investigation of Power-Aware IEEE 802.11 Performance in Multi-hop Ad Hoc Networks. In: Zhang, H., Olariu, S., Cao, J., Johnson, D.B. (eds.) MSN 2007. LNCS, vol. 4864, pp. 409–420. Springer, Heidelberg (2007)
2. Barowski, Y., Biaz, S., Agrawal, P.: Towards the performance analysis of IEEE 802.11 in multi-hop ad-hoc networks. In: Proceedings of IEEE Wireless Communications and Networking Conference (WCNC), pp. 100–106 (March 2005)
3. Bianchi, G.: Performance analysis of the IEEE 802.11 distributed coordination function. IEEE Journal on Selected Areas in Communications 18(3), 535–547 (2000)
4. Camp, J., Aryafar, E., Knightly, E.: Coupled 802.11 Flows in Urban Channels: Model and Experimental Evaluation. In: INFOCOM, San Diego, CA (March 2010)
5. Kherani, A., El-Khoury, R., El-Azouzi, R., Altman, E.: Stability-throughput trade-off and routing in multi-hop wireless ad-hoc networks. Computer Networks 52(7), 1365–1389 (2008)
6. Kumar, A., Altman, E., Miorandi, D., Goyal, M.: New insights from a fixed point analysis of single cell IEEE 802.11 WLANs. In: INFOCOM, pp. 1550–1561 (2005)
7. Li, N., Hou, J.C., Sha, L.: Design and analysis of a MST-based distributed topology control algorithm for wireless ad-hoc networks. IEEE Transactions on Wireless Communications 4(3), 1195–1207 (2005)
8. Medepalli, K., Tobagi, F.A.: Towards performance modeling of IEEE 802.11 based wireless networks: A unified framework and its applications. In: Proceedings of IEEE INFOCOM (2006)
9. Ramaiyan, V., Kumar, A., Altman, E.: Fixed point analysis of single cell IEEE 802.11e WLANs: uniqueness, multistability and throughput differentiation. SIGMETRICS Performance Evaluation Review 33(1), 109–120 (2005)



10. Sakurai, T., Vu, H.L.: Mac access delay of IEEE 802.11 DCF. *IEEE Transactions on Wireless Communications* 6(5), 1702–1710 (2007)
11. Vassis, D., Kormentzas, G.: Performance analysis of IEEE 802.11 ad hoc networks in the presence of exposed terminals. *Ad Hoc Networks* 6(3), 474–482 (2008)
12. Yang, Y., Hou, J.C., Kung, L.C.: Modeling the effect of transmit power and physical carrier sense in multi-hop wireless networks. In: *Proceedings of IEEE INFOCOM* (2007)
13. El-Azouzi, R., Sabir, E., Raiss-El-Fenni, M., Samanta, S.K.: A Complete Multi-layered Framework for IEEE 802.11e Multi-hop Ad hoc Networks, <http://lia.univ-avignon.fr/fileadmin/documents/Users/Intranet/chercheurs/sabir/802eTechReport.pdf>